Interbilayer-crosslinked multilamellar vesicles as synthetic vaccines for potent humoral and cellular immune responses

Published in final edited form as:
Nat Mater. 2011 March ; 10(3): 243–251. doi:10.1038/nmat2960.

Interbilayer-Crosslinked Multilamellar Vesicles as Synthetic Vaccines for Potent Humoral and Cellular Immune Responses

James J. Moon[1,2], **Heikyung Suh**[1,2,6], **Anna Bershteyn**[1], **Matthias T. Stephan**[1,2], **Haipeng Liu**[1,2], **Bonnie Huang**[2], **Mashaal Sohail**[2], **Samantha Luo**[1], **Soong Ho Um**[1,2], **Htet Khant**[3], **Jessica T. Goodwin**[3], **Jenelyn Ramos**[3], **Wah Chiu**[3], and **Darrell J. Irvine**[1,2,4,5,6]

[1]Department of Materials Science and Engineering, Massachusetts Institute of Technology (MIT), Cambridge, MA, USA

[2]Department of Biological Engineering, MIT, Cambridge, MA, USA

[3]National Center for Macromolecular Imaging, Verna and Marrs McLean Department of Biochemistry and Molecular Biology, Baylor College of Medicine, Houston, TX, USA

[4]Koch Institute for Integrative Cancer Research, MIT, Cambridge, MA, USA

[5]Ragon Institute of MGH, MIT, and Harvard, Boston, MA, USA

[6]Howard Hughes Medical Institute, Chevy Chase, MD, USA

Abstract

Vaccines based on recombinant proteins avoid toxicity and anti-vector immunity associated with live vaccine (e.g., viral) vectors, but their immunogenicity is poor, particularly for $CD8^+$ T-cell (CD8T) responses. Synthetic particles carrying antigens and adjuvant molecules have been developed to enhance subunit vaccines, but in general these materials have failed to elicit CD8T responses comparable to live vectors in preclinical animal models. Here, we describe interbilayer-crosslinked multilamellar vesicles (ICMVs) formed by crosslinking headgroups of adjacent lipid bilayers within multilamellar vesicles. ICMVs stably entrapped protein antigens in the vesicle core and lipid-based immunostimulatory molecules in the vesicle walls under extracellular conditions, but exhibited rapid release in the presence of endolysosomal lipases. We found that these antigen/adjuvant-carrying ICMVs form an extremely potent whole-protein vaccine, eliciting endogenous T-cell and antibody responses comparable to the strongest vaccine vectors. These materials should enable a range of subunit vaccines and provide new possibilities for protein therapeutic delivery.

Currently licensed vaccine adjuvants (e.g., aluminum hydroxide and the oil-in-water emulsion MF59) promote immunity by primarily eliciting humoral immune responses, without stimulating cellular immunity1›2. As strong $CD8^+$ T cell (CD8T) responses may be required for vaccines against cancer or intracellular pathogens such as HIV, malaria, and hepatitis C, there is great interest in technologies to promote concerted humoral and cellular

Correspondence should be addressed to D.J.I. (djirvine@mit.edu).

AUTHOR CONTRIBUTIONS

J.J.M. and D.J.I. designed the experiments. J.J.M. performed the experiments; H.S. assisted in the *in vivo* characterization and immunization studies. A.B., H.K., J.T.G., J.R., and W.C. contributed cryoelectron microscope imaging. M.T.S. and S.H.U. contributed experimental suggestions. H.L., B.H., M.S., and S.L. provided technical support. J.J.M. and D.J.I. analyzed the data and wrote the paper.

The authors declare no competing financial interests.

immune responses[3,4]. To this end, engineered live vaccine vectors such as non-replicating recombinant viruses have been developed[5–7], which can induce both robust antibody responses and massive expansion of functional antigen-specific $CD8^+$ T-cells in murine models. However, safety concerns with live vectors and anti-vector immunity can complicate live vector vaccine design[7]. Pre-existing vector-specific immune responses have reduced the immunogenicity of live vector-based vaccines in clinical trials[8], and the immune response raised against live vectors following a priming immunization can render booster immunizations using the same vector problematic[7].

In contrast, non-living synthetic vaccines delivering defined antigens can be rationally designed to avoid anti-vector immunity[9]. Such "subunit" vaccines are composed of one or a few selected recombinant proteins or polysaccharides normally present in the structure of the target pathogen. However, subunit vaccines elicit poor or non-existent CD8T responses, due to the low efficiency of cross-presentation (the uptake and processing of extracellular antigen by immune cells for presentation on class I MHC molecules to naive $CD8^+$ T-cells)[10]. To promote cross-presentation, synthetic particles loaded with protein antigens and defined immunostimulatory molecules have been used[11–17], mimicking in a reductionist fashion the cues provided to the immune system during infection by pathogens. Liposomes are particularly attractive materials for this application, due to their low toxicity and immunogenicity, track record of safety in clinical use, ease of preparation, and proven manufacturability at commercial scales[18,19]. Lipid vesicles in the form of unilamellar, multilamellar, or polymerized vesicles have been tested as vaccine delivery materials, with some success[19–23]. Antigens entrapped in lipid vesicles are cross-presented *in vivo*[19,24,25], and liposomal protein vaccines have been shown to elicit protective T-cell-mediated anti-microbial and anti-tumor immune responses in small-animal models[23,26,27]. However, for diseases such as HIV and cancer, it is currently believed that extremely potent T-cell responses (in concert with humoral immunity) will be required to control the virus/tumors, and therefore, more potent T-cell vaccines are still sought[3,4].

A potential factor influencing the potency of lipid vesicles in vaccine delivery is their limited stability in the presence of serum components. For liposomal cargos that can be processed at high temperature or loaded by diffusion through pre-formed vesicle membranes, enhanced vesicle stability can be achieved by using high-T_m lipids, especially when combined with cholesterol and/or PEGylation[28]. Uni-and multi-lamellar vesicles have also been stabilized by polymerizing reactive headgroups at the surface of bilayers[29], polymerizing reactive groups in phosholipid acyl tails[20,29], or polymerizing hydrophobic monomers adsorbed into the hydrophobic interior of membranes[30]. Common to each of these approaches is the concept of polymerizing components in the plane of the bilayer. However, finding polymerization chemistries that can be carried out in mild conditions compatible with vaccine antigens is challenging[20].

Here we describe a new class of lipid drug carriers, interbilayer-crosslinked multilamellar vesicles (ICMVs), formed by stabilizing multilamellar vesicles with short covalent crosslinks linking lipid headgroups across the opposing faces of adjacent tightly-stacked bilayers within the vesicle walls. ICMVs encapsulated and stably retained high levels of proteins, releasing entrapped cargo very slowly when exposed to serum (over 30 days) compared to simple liposomes or multilamellar vesicles (MLVs) of the same lipid composition. However, these vesicles were quickly degraded in the presence of lipases normally found at high levels within intracellular compartments[31]. Using this novel vesicle structure to co-entrap high levels of a model protein antigen (ovalbumin, OVA) and a lipid-like immunostimulatory ligand (monophosphoryl lipid A, MPLA), we carried out immunization studies in mice and found that ICMVs elicited robust antibody titers ~1000-fold greater than simple liposomes and ~10-fold greater than MLVs of identical lipid

compositions. Unlike live vectors that are often only effective for a single injection administered to a vector-naïve individual7, these synthetic vesicles triggered steadily increasing humoral and $CD8^+$ T-cell responses following repeated administrations, with antigen-specific T-cells expanding to a peak of nearly 30% of the total $CD8^+$ T-cells in blood following a prime and two booster immunizations. These new materials may thus open the door to subunit vaccines that are both safe and highly effective for generating both humoral and cellular immunity.

We introduced covalent crosslinks between functionalized lipid headgroups of adjacent, apposed bilayers within preformed MLVs to form ICMVs (Fig. 1a): In a typical synthesis, dried phospholipid films containing DOPC, anionic DOPG, and the anionic maleimide-headgroup lipid MPB in a 4:1:5 molar ratio were hydrated and sonicated to form simple liposomes (step (i)). Divalent cations (e.g., Mg^{2+}) were added to the liposomes to induce vesicle fusion and the formation of MLVs as reported previously32 (step (ii)). To introduce crosslinks between adjacent bilayers in the MLVs, dithiothreitol (DTT) was then added to the vesicle suspension to act as a membrane-permeable crosslinker, forming a covalent linkage between maleimide headgroups of apposed membranes brought into proximity by the cation salt bridges formed between vesicle layers (step (iii)). PEGylation is a well-known strategy to increase the serum stability and blood circulation half-life of lipid vesicles18. Thus as a final step, the vesicles were washed and residual maleimide groups exposed on the external surfaces of the particles were capped with thiol-terminated PEG (step (iv)).

The diameter/polydispersity of the particles will determine the cell types capable of internalizing these particles33, while the number of bilayers comprising the vesicle walls would be expected to impact the stability of the vesicles and their ability to retain/slowly release cargos in the presence of serum. To evaluate these properties and better understand the process of ICMV formation, we characterized the products at each step of the synthesis: The initial liposomes formed by sonication (step (i)) had hydrodynamic diameters of ~190 nm, and the size increased slightly to ~ 240 nm following Mg^{2+}-mediated vesicle fusion (step (ii)) and subsequent DTT "stapling" of the bilayers (step (iii), Table 1). The resulting ICMVs showed a monomodal, relatively narrow size distribution (comparable to common lipid vesicle or polymer nanoparticle preparations12,21), and there was no evidence for gross aggregation of particles during the crosslinking step from dynamic light scattering (DLS) or cryoelectron microscopy (Fig. 1a, b, and Table 1). Addition of thiol-terminated PEG to DTT-treated vesicles quenched remaining detectable maleimide groups on the surfaces of MLVs and introduced PEG chains on ~2 mol% of the surface-exposed lipids of ICMVs without significantly altering particle diameters (Supplementary Fig. S1a, b, and Table 1). PEGylated ICMVs stored at 4°C or 37°C in PBS remained stable over 7 days, and they were amenable to lyophilization with 3% sucrose added as an excipient34, highlighting their compatibility with long-term storage conditions (Table 1 and data not shown). We imaged the initial liposomes, Mg^{2+}-fused MLVs, and the final ICMVs by cryoelectron microscopy (Fig. 1a), and saw that crosslinking with DTT led to the formation of vesicles with thick multilamellar walls composed of tightly stacked bilayers resolved as ~4–5 nm electron-dense striations. The median number of bilayers per particle was 4.4 (interquartile range [IQR], 3.3–6.9), and the median particle radius to lipid wall thickness ratio was 3.8 (IQR, 2.4–6.8) (Fig. 1c, d). Interestingly, the majority of ICMVs had vesicle walls composed of concentric bilayers, although a few examples of ICMVs with surface defects in the form of incomplete external lipid layers could also be found (Supplementary Fig. S2). Consistent with the increased lamellarity of the vesicles following cation-mediated fusion and DTT crosslinking observed by electron microscopy imaging, the fraction of lipids exposed on the external surfaces of the vesicles decreased in steps (ii) and (iii) of the synthesis, as measured by a bulk dye-quenching lamellarity assay35 (Table 1). Chemical

evidence for crosslinking between the maleimide-lipids following DTT treatment was found in thin-layer chromatography and MALDI-TOF measurements on ICMVs (Supplementary Fig. S3 and data not shown). Importantly, both the particle size and individual lamellarity distributions were monomodal, with less than 3 % contaminating unilamellar vesicles and no large aggregates, which could skew the functional properties (e.g., protein release) of the particles. The ICMVs have a size that should be avidly taken up by monocytes and dendritic cells36, and a crosslinked multilamellar wall structure that will stabilize protein entrapment compared to traditional unilamellar or multilamellar liposomes.

Analysis of the conditions required to form stable vesicles provided insight into the mechanisms of ICMV formation. Following interbilayer-crosslinking, ICMVs could be collected by centrifuging at 14,000 × *g* for 4 min ("low-speed conditions"), whereas simple liposomes or MLVs of identical lipid composition required ultracentrifugation to pellet. Using the mass of particles collected by low-speed centrifugation as a surrogate measure of crosslinked vesicle yield, we found that both divalent cation-mediated fusion (Fig. 1a step (ii), either Mg^{2+} or Ca^{2+}) and DTT treatment (step (iii)) were required for ICMV formation (Table 2; entries 1–3). Precursor vesicles treated with either Mg^{2+} or DTT alone even at 10X molar excess relative to maleimide groups did not generate significant yields of particles (Table 2, entries 4–6). In addition, at least 25 mol% MPB was required to form ICMVs (Table 1, entries 1, 7–9); the high level of reactive headgroups required for substantial ICMV yield may reflect competition between intra- (between headgroups on the same bilayer) and inter-bilayer crosslink formation. DTT could be replaced with DPDPB, another membrane-permeable dithiol, but not with 2 kDa PEG-dithiol (Supplementary Fig. S4 and Table 2 entries 10, 11). ICMVs could also be formed using only DOPC and MPB lipids, or using cationic DOTAP in place of DOPG (data not shown). As an alternative method to form ICMVs, maleimide-dithiol crosslinking could be replaced with bio-orthogonal click chemistry, employing alkyne-terminated lipids for vesicle formation and diazides for crosslinking37,38 (Supplementary Fig. S5). Thus, interbilayer-crosslinking for the formation of stabilized vesicles is a general strategy that can be adapted to other lipid/crosslinker chemistries. Based on their high synthetic yield and colloidal stability, we chose to focus on PEGylated ICMVs with a lipid composition of DOPC:DOPG:MPB in a 4:1:5 molar ratio for further testing as protein/vaccine delivery vehicles.

To test the suitability of ICMVs for protein delivery, we examined the entrapment of several globular proteins: SIV-gag, an HIV vaccine antigen; FLT-3L, a therapeutic cytokine; and ovalbumin (OVA), a model vaccine antigen. Protein encapsulation was achieved by rehydrating dried lipids with protein solutions in step (i) of the synthesis (Fig. 1a). The amount of encapsulated protein increased at each step of the ICMV preparation (Fig. 2a), which may reflect additional protein entrapment occurring as vesicle fusion occurs in both steps (ii) and (iii). Protein entrapment in ICMVs was not mediated by conjugation of thiols on the cargo proteins with the maleimide-functionalized lipid vesicles, as OVA pre-reduced with TCEP and treated with ethyl-maleimide to block all thiol groups on the protein was encapsulated in ICMVs at levels similar to unmodified protein (76.1 ± 6.3% vs. 83.3 ± 8.4 % for capped-thiol- vs. unmodified OVA; $p = 0.17$). We also confirmed that disulfide linkages in model protein cargos were not reduced by the DTT crosslinker during the vesicle formation process and that ICMV encapsulation did not trigger protein aggregation (Supplementary Fig. S6). To directly compare the efficiency and quantity of protein loading achieved with ICMVs to two of the most common types of drug delivery vehicles39–41, we compared encapsulation of OVA in liposomes, PLGA nanoparticles, and ICMVs: Using a model stable lipid composition comprised of phosphocholine, PEG-lipid, and cholesterol42, we formed DRVs as one of the most efficient aqueous entrapment approaches for liposomes43, and prepared OVA-loaded PLGA particles using a double-emulsion solvent-evaporation process44. ICMVs exhibited superior encapsulation efficiency (~75 %)

compared to either DRVs or PLGA particles (2-, and 4-fold increases, respectively; Fig. 2b), and the amount of OVA encapsulated per total particle mass (~325 μg OVA per mg of particles) was increased in ICMVs by 1.8-, and 9-fold compared to DRVs or PLGA particles, respectively (Fig. 2c). Thus, ICMVs appear to be effective for encapsulating a variety of globular proteins, and, at least for the model antigen OVA, ICMVs loaded protein more efficiently than common alternative protein carriers.

We next determined whether interbilayer crosslinking enabled lipid vesicles to retain biodegradability while increasing protein retention in the presence of serum. OVA was loaded into PEGylated liposomes, Mg^{2+}-fused MLVs, or ICMVs all with the same lipid composition, and the kinetics of protein release at 37°C in media containing 10% fetal calf serum were quantified. Unilamellar liposomes quickly released their entire payload of entrapped OVA within ~2 days, while multilamellar Mg^{2+}-fused MLVs released ~50% of their entrapped cargo over the same time period (Fig. 2d). However, ICMVs showed a significantly enhanced retention of protein, releasing only ~25% of their cargo by one week, and ~90% after 30 days (Fig. 2d). Notably, ICMVs also released protein significantly more slowly than unilamellar liposomes stabilized by the inclusion of cholesterol42 (Fig. 2d). The crosslinked vesicles also retained ~95% of their entrapped protein when stored in PBS at 4°C for over 30 days (Fig. 2e). We also examined protein release from ICMVs in conditions modeling intracellular compartments: vesicles incubated in reducing or acidic conditions for 1 day at 37°C retained > 95% of entrapped OVA, whereas incubation with phospholipase A led to release of > 90% OVA and rapid vesicle degradation (Fig. 2e). Thus, ICMVs exhibit enhanced stability in the presence of serum compared to traditional liposomal formulations, but rapidly break down in the presence of enzymes that are present within intracellular endolysosomal compartments31, providing a mechanism for triggered intracellular release of cargo following internalization by cells. Although some protein degradation within vesicles might be possible upon administration *in vivo* prior to internalization by cells, critical uptake and processing of antigen will occur in the first few days after immunization in vaccine delivery45, when such degradation processes should be minimal.

We hypothesized that the unique structure of ICMVs, with efficient retention of encapsulated protein antigens in the extracellular environment but rapid release in endosomes/lysosomes, would provide enhanced vaccine responses. To generate vaccine ICMVs, we prepared vesicles carrying the model antigen OVA (OVA-ICMVs) and mixed these vesicles with the molecular adjuvant monophosphoryl lipid A (MPLA). MPLA is an FDA-approved agonist for Toll-like receptor (TLR) 4 expressed by dendritic cells, B-cells, and innate immune cells, and potently amplifies vaccine responses1,46. Antigen-loaded ICMVs mixed with MPLA promoted upregulation of costimulatory molecules on splenic and bone-marrow dendritic cells (DCs) *in vitro*, compared to DCs pulsed with ICMVs without MPLA (Fig. 3a and Supplementary Fig. S7). DCs pulsed with ICMVs cross-presented peptides derived from OVA with greatly enhanced efficiency compared to those pulsed with soluble OVA (with or without added MPLA), as determined by staining DCs with the 25-D1.16 mAb that recognizes the SIINFEKL peptide ($OVA_{257–264}$) complexed with MHC class I H-$2K^b$ molecules ($p < 0.001$, compared to soluble OVA or ICMVs-loaded with irrelevant antigen [vivax malaria protein, VMP], Fig. 3b). Splenic DCs incubated with OVA-ICMVs + MPLA triggered robust proliferation of OVA-specific naïve OT-1 $CD8^+$ T-cells *in vitro*, as assessed by a carboxyfluorescein succinimidyl ester (CFSE) dilution assay. In contrast, weak T-cell responses were detected when DCs were pulsed with equivalent doses of soluble OVA and MPLA, empty ICMVs, or VMP-ICMVs, indicating the specificity of the T-cell responses elicited by ICMVs (Fig. 3c). These results suggest that addition of MPLA allows equivalent DC activation by ICMVs or soluble OVA, but ICMVs trigger enhanced cross-presentation of the antigen, as expected for particulate antigen delivery.

To determine the influence of vesicle structure on the immune response *in vivo*, we vaccinated C57Bl/6 mice with equivalent doses of OVA, MPLA, and lipids (10 μg, 0.1 μg, and 142 μg, respectively) in the form of PEGylated unilamellar liposomes, MLVs, or ICMVs. Seven days after immunization, we assessed the strength of the endogenous $CD8^+$ T-cell response by analyzing the frequency of OVA peptide-MHC $tetramer^+$ (antigen-specific) $CD8^+$ T-cells among peripheral blood mononuclear cells (PBMCs) by flow cytometry, and found a trend toward increasing T-cell responses in the order soluble OVA < liposomes < Mg^{2+}-fused MLVs < ICMVs (Fig. 4a). At 3 weeks post-immunization, Mg^{2+}-fused MLVs elicited ~100-fold greater OVA-specific IgG titers in the sera of the animals compared to soluble OVA or unilamellar liposomes. However, ICMV immunization generated a substantially stronger humoral response, ~1000-fold and ~10-fold greater than the soluble OVA ($p < 0.01$) and non-crosslinked MLV immunizations ($p < 0.05$), respectively (Fig. 4b). Thus, the stabilized structure of ICMVs promoted both T-cell and antibody responses. Enhanced T-cell and antibody responses to immunization with ICMVs compared to other formulations, could be attributed to improved antigen delivery to antigen-presenting cells (APCs), enhanced activation of DCs, enhanced antigen cross-presentation (as seen *in vitro*), or a combination of these factors. To distinguish between these possibilities, mice were immunized with fluorophore-conjugated OVA mixed with MPLA as a soluble, liposomal, or ICMV formulation, and the draining inguinal lymph node cells that internalized OVA were assessed on day 2. OVA delivered by ICMVs was readily detected in total DCs, macrophages, and plasmacytoid ($CD11c^+B220^+$) DCs in the draining lymph nodes (dLNs), while soluble and liposomal formulations showed fluorescence barely above background ($p < 0.01$, Fig. 4c, d). Repeating this analysis with unlabeled OVA, we found that administration of OVA-ICMVs with MPLA triggered a minor enhancement of co-stimulatory marker and MHC-II expression among DCs in dLNs compared to soluble or liposomal OVA + MPLA (Fig. 4e and Supplementary Fig. S8). However, using the 25-D1.16 antibody to detect OVA peptide presentation, we readily detected OVA peptide-MHC complexes on DCs in the dLNs following ICMV immunization, whereas soluble OVA or liposomal OVA injections did not give staining above the expected background cross-reactivity of 25-D1.16 with self-peptide MHC complexes47 (Fig. 4f). All together, these results suggest that improved retention of entrapped antigen in the crosslinked multilamellar structures of ICMVs leads to enhanced antigen delivery to APCs, followed by enhanced cross-presentation.

The multilamellar structure of ICMVs offers the opportunity to sequester not only protein antigen (in the aqueous core) but also lipophilic molecules (in the vesicle walls). We thus tested whether embedding MPLA throughout the walls of the ICMVs would impact the immune response *in vivo*, by allowing better retention of MPLA together with antigen in the vesicles. The TLR agonist was incorporated throughout the vesicle layers by co-dissolving MPLA with the other lipids in the first step of the synthesis (int-MPLA ICMVs), and we compared these vesicles to ICMVs carrying the same amount of MPLA incorporated only on the vesicle surfaces via a post-insertion approach (ext-MPLA ICMVs, Fig. 5a, Supplementary Methods). Mice were immunized s.c. with OVA (10 μg) and MPLA (0.1 μg or 1.0 μg) in ICMVs or soluble form, and boosted on d21 and d35 with the same formulations. As shown in Fig. 5b, immunizations using the low dose of MPLA led to a barely detectable antibody response against soluble OVA even following two boosts, while both int-MPLA and ext-MPLA ICMVs elicited strong anti-OVA serum IgG titers by d56. An IgG response to soluble OVA could be obtained using 10-fold more MPLA, but int-MPLA ICMVs with 1.0 μg MPLA elicited higher titers than soluble protein (~13-fold greater on d56). On the other hand, we did not observe any significant level of antibodies directed against lipid components of ICMVs throughout these immunization studies (data not shown).

Embedding MPLA in the multilayers of ICMVs had a more striking effect on the $CD8^+$ T-cell response to vaccination. Soluble OVA mixed with 0.1 μg MPLA elicited barely detectable antigen-specific T-cell expansion as assessed by tetramer staining on PBMCs; ext-MPLA ICMV delivery led to a 2.5-fold increased $tetramer^+$ T-cell population by d41 (Fig. 5c, $p < 0.05$). Adding 10-fold more MPLA allowed soluble OVA immunizations to eventually reach T-cell responses equivalent to ext-MPLA ICMVs following boosting. By contrast, immunization with int-MPLA ICMVs elicited dramatically stronger $CD8^+$ T-cell responses that continued to expand following each boost, achieving a peak 28% $tetramer^+$ T-cells in the $CD8^+$ T-cell population by d41 (5-fold greater than ext-MPLA ICMVs ($p < 0.05$) and 14-fold greater than soluble OVA+MPLA ($p < 0.01$) Fig. 5c). Notably, int-MPLA ICMVs elicited overall a significantly higher frequency of $tetramer^+CD44^+CD62L^+$ cells ($p < 0.01$, Fig. 5d), a phenotype for central memory T-cells known to confer long-lived protection against pathogens and tumors48. Antigen specific T-cells elicited by int-MPLA ICMVs persisted even after one month after the final boosting, with ~11% $tetramer^+$ T-cells among $CD8^+$ T-cells (3-fold and 8-fold greater than ext-MPLA ICMVs and soluble OVA +MPLA, respectively, $p < 0.05$ for both, Fig. 5c). To test the functionality of T-cells expanded by these immunizations, we assessed the ability of $CD8^+$ T-cells from peripheral blood to produce interferon-γ (IFN-γ) upon restimulation *ex vivo* on d49. Mice immunized with int-MPLA ICMVs had much higher levels of IFN-γ-competent T-cells than mice receiving ext-MPLA ICMVs or soluble OVA-immunizations ($p < 0.05$, Fig. 5e). To our knowledge, in terms of the degree of antigen-specific T-cell expansion, persistence of memory cells, and IFN-γ functionality, this is one of the strongest endogenous T-cell responses ever reported for a protein vaccine, comparable to strong live vectors such as recombinant viruses5,6. Notably, this is achieved via "homologous" boosting, repeated immunization with the same particle formulation, a strategy that cannot be used with many live vectors due to immune responses raised against the pathogen-based delivery vector itself7.

These studies demonstrate the synthesis of a new class of submicron particle reagents based on crosslinked multilamellar lipid vesicles, which combine a number of attractive features for biomedical applications; the particle synthesis does not require exposure of protein cargos to organic solvents, the lipid basis of the particles makes them inherently biodegradable to metabolizable byproducts, the phospholipid shell enables modular entrapment of both lipophilic and hydrophilic cargos, proteins are encapsulated at very high levels per mass of particles, and protein release from the particles can be sustained over very long durations. These results suggest ICMVs may be a very effective vehicle for delivering biomacromolecules, and in particular, for vaccine applications. The ability to achieve such strong combined T-cell and antibody responses using a synthetic particle vaccine could open up new possibilities for vaccination in the setting of infectious disease and cancer.

MATERIALS AND METHODS

Synthesis of ICMVs

1.26 μmol of lipids in chloroform (typical lipid composition: DOPC(1,2-Dioleoyl-*sn*-Glycero-3-Phosphocholine):DOPG(1,2-di-(9Z-octadecenoyl)-sn-glycero-3-phospho-(1'-rac-glycerol)): MPB (1,2-dioleoyl-*sn*-glycero-3-phosphoethanolamine-N-[4-(p-maleimidophenyl) butyramide) = 4:1:5 molar ratio, all lipids from Avanti Polar Lipids, Alabaster, AL) were dispensed to glass vials, and the organic solvents were evaporated under vacuum overnight to prepare dried thin lipid films. The lipid films were rehydrated in 10 mM bis-tris propane at pH 7.0 with cargo proteins for 1 hr with rigorous vortexing every 10 min, and then sonicated in alternating power cycles of 6 watts and 3 watts in 30s intervals for 5 min on ice (Misonix Microson XL probe tip sonicator, Farmingdale, NY). The liposomes formed in this first step were induced to undergo fusion by addition of divalent

cations such as Mg^{2+} and Ca^{2+} at a final concentration of 10 mM. The resulting MLVs were incubated with 1.5 mM DTT (maleimide:DTT molar ratio of 2:1) for 1 hr at 37°C to conjugate opposing bilayers of maleimide-functionalized lipids and form crosslinked ICMVs; the resulting vesicles were recovered by centrifugation at 14,000 ×*g* for 4 min, and washed twice with deionized water. For PEGylation, the particles were incubated with 2 kDa PEG-thiol (Laysan Bio, Arab, AL) in a 1.5-fold molar excess of PEG-SH to maleimide groups for 1 hr at 37°C. The resulting particles were centrifuged and washed 3X with deionized water. The final products were either stored in PBS at 4°C or lyophilized in the presence of 3% sucrose as a cryoprotectant and stored at −20°C. For some assays, simple liposomes or Mg-fused MLVs were harvested prior to crosslinking with ultracentrifugation at 115 k × *g* using an Optima ultracentrifuge for 6 hrs (Beckman Coulter).

In vitro protein loading and drug release

For encapsulation studies, ovalbumin (OVA, Worthington, Lakewood, NJ), SIV-gag (Advanced Bioscience Laboratories, Kensington, MD), and FLT-3L (Peprotech, Rocky Hill, NJ) were labeled with Alexa-Fluor 555 (Invitrogen, Carlsbad, CA) for direct fluorometric quantification of the amount of protein entrapped. OVA was also encapsulated in DRVs and PLGA nanoparticles as described previously43,44. In some experiments, ICMVs were loaded with a recombinant vivax malaria protein (VMP) as an irrelevant antigen control49 (provided by Dr. Anjali Yadava, Walter Reed Army Institute of Research). Capped-thiol OVA was prepared by incubating 1 mg of OVA with 1.5 mM TCEP for 1 hr at RT, followed by incubation with 1.5 mM ethyl-maleimide (Pierce, Rockford, IL) at 37 °C for 1hr. The extent of thiol protection was > 95% as assessed with Ellman's assay50. Release of OVA labeled with Alexa-Fluor 555 from lipid vesicles was quantified in RPMI media supplemented with 10% fetal calf serum at 37°C using dialysis membranes with MW cutoff of 100 kDa. At regular intervals, the releasing media were removed for quantification of fluorescence, and an equal volume of fresh media were replaced for continued monitoring of drug release. Residual OVA remaining at the end of the time-course was determined by lipid extraction of vesicles with 1% Triton X-100 treatment and measuring released protein by fluorescence spectrophotometry. OVA release assays were also performed in Hank's buffered saline solution supplemented with 500 ng/ml of phospholipase A (Sigma, St. Louis, MO). To examine stability of encapsulated cargo molecules, monoclonal rat IgG encapsulated in ICMVs was retrieved with 1% triton X-100 treatment and analyzed with SDS-PAGE under non-reducing conditions with silver staining (Pierce).

Vaccination study with ICMVs

Groups of C57Bl/6 mice (Jackson Laboratories) were immunized s.c. in the tail base with indicated doses of OVA (with or without TLR agonists, MPLA). Frequencies of OVA-specific $CD8^+$ T-cells and their phenotypes elicited by immunization were determined by flow cytometry analysis of PBMCs at selected time points following staining with DAPI (to discriminate live/dead cells), anti-CD8α, anti-CD44, anti-CD62L, and SIINFEKL/H-$2K^b$ peptide-MHC tetramers (Becton Dickinson). To assess functionality of primed $CD8^+$ T-cells, PBMCs were stimulated *ex vivo* with 1 μM OVA-peptide SIINFEKL for 6 hrs with GolgiPlug (Becton Dickinson), fixed, permeabilized, stained with anti- IFN-γ and CD8α, and analyzed by flow cytometry. Anti-OVA IgG titers, defined as the dilution of sera at which 450 nm OD reading is 0.5, were determined by ELISA analysis of sera from immunized mice. Animals were cared for following NIH, state, and local guidelines.

Statistical analysis

Statistical analysis was performed with Jmp 5.1 (SAS Institute Inc, Cary, NC). Data sets were analyzed using one- or two-way analysis of variance (ANOVA), followed by Tukey's

HSD test for multiple comparisons. p-values less than 0.05 were considered statistically significant. All values are reported as mean ± s.e.m.

Supplementary Material

Refer to Web version on PubMed Central for supplementary material.

Acknowledgments

This work was supported in part by the Ragon Institute of MGH, MIT, and Harvard, the Gates Foundation, the Dept. of Defense (contract W911NF-07-D-0004), and NIH (P41RR002250 and RC2GM092599). The authors would like to thank Dr. Anjali Yadava for providing the VMP antigen. D.J.I. is an investigator of the Howard Hughes Medical Institute.

REFERENCES

1. Guy B. The perfect mix: recent progress in adjuvant research. Nat. Rev. Microbiol. 2007; 5:505–517. [PubMed: 17558426]
2. Perrie Y, Mohammed AR, Kirby DJ, McNeil SE, Bramwell VW. Vaccine adjuvant systems: enhancing the efficacy of sub-unit protein antigens. Int. J. Pharm. 2008; 364:272–280. [PubMed: 18555624]
3. Reed SG, Bertholet S, Coler RN, Friede M. New horizons in adjuvants for vaccine development. Trends Immunol. 2009; 30:23–32. [PubMed: 19059004]
4. Walker BD, Burton DR. Toward an AIDS vaccine. Science. 2008; 320:760–764. [PubMed: 18467582]
5. Haglund K, et al. Robust recall and long-term memory T-cell responses induced by prime-boost regimens with heterologous live viral vectors expressing human immunodeficiency virus type 1 Gag and Env proteins. J. Virol. 2002; 76:7506–7517. [PubMed: 12097563]
6. Flatz L, et al. Development of replication-defective lymphocytic choriomeningitis virus vectors for the induction of potent CD8+ T cell immunity. Nat. Med. 2010; 16:339–345. [PubMed: 20139992]
7. Brave A, Ljungberg K, Wahren B, Liu MA. Vaccine delivery methods using viral vectors. Mol. Pharm. 2007; 4:18–32. [PubMed: 17274663]
8. Priddy FH, et al. Safety and immunogenicity of a replication-incompetent adenovirus type 5 HIV-1 clade B gag/pol/nef vaccine in healthy adults. Clin. Infect. Dis. 2008; 46:1769–1781. [PubMed: 18433307]
9. Hubbell JA, Thomas SN, Swartz MA. Materials engineering for immunomodulation. Nature. 2009; 462:449–460. [PubMed: 19940915]
10. Heath WR, Carbone FR. Cross-presentation in viral immunity and self-tolerance. Nat. Rev. Immunol. 2001; 1:126–134. [PubMed: 11905820]
11. Kwon YJ, James E, Shastri N, Frechet JM. In vivo targeting of dendritic cells for activation of cellular immunity using vaccine carriers based on pH-responsive microparticles. Proc. Natl. Acad. Sci. USA. 2005; 102:18264–18268. [PubMed: 16344458]
12. Hamdy S, et al. Enhanced antigen-specific primary CD4+ and CD8+ responses by codelivery of ovalbumin and toll-like receptor ligand monophosphoryl lipid A in poly(D,L-lactic-co-glycolic acid) nanoparticles. J. Biomed. Mater. Res. A. 2007; 81:652–662. [PubMed: 17187395]
13. Heit A, Schmitz F, Haas T, Busch DH, Wagner H. Antigen co-encapsulated with adjuvants efficiently drive protective T cell immunity. Eur. J. Immunol. 2007; 37:2063–2074. [PubMed: 17628858]
14. Schlosser E, et al. TLR ligands and antigen need to be coencapsulated into the same biodegradable microsphere for the generation of potent cytotoxic T lymphocyte responses. Vaccine. 2008; 26:1626–1637. [PubMed: 18295941]
15. Heffernan MJ, Kasturi SP, Yang SC, Pulendran B, Murthy N. The stimulation of CD8+ T cells by dendritic cells pulsed with polyketal microparticles containing ion-paired protein antigen and poly(inosinic acid)-poly(cytidylic acid). Biomaterials. 2009; 30:910–918. [PubMed: 19036430]

16. Demento SL, et al. Inflammasome-activating nanoparticles as modular systems for optimizing vaccine efficacy. Vaccine. 2009; 27:3013–3021. [PubMed: 19428913]
17. Reddy ST, et al. Exploiting lymphatic transport and complement activation in nanoparticle vaccines. Nat. Biotechnol. 2007; 25:1159–1164. [PubMed: 17873867]
18. Torchilin VP. Recent advances with liposomes as pharmaceutical carriers. Nat. Rev. Drug Discov. 2005; 4:145–160. [PubMed: 15688077]
19. Gregoriadis G, Gursel I, Gursel M, McCormack B. Liposomes as immunological adjuvants and vaccine carriers. J. Control. Release. 1996; 41:49–56.
20. Jeong JM, Chung YC, Hwang JH. Enhanced adjuvantic property of polymerized liposome as compared to a phospholipid liposome. J. Biotechnol. 2002; 94:255–263. [PubMed: 11861084]
21. Vangala A, et al. Comparison of vesicle based antigen delivery systems for delivery of hepatitis B surface antigen. J. Control. Release. 2007; 119:102–110. [PubMed: 17331610]
22. Steers NJ, Peachman KK, McClain S, Alving CR, Rao M. Liposome-encapsulated HIV-1 Gag p24 containing lipid A induces effector CD4+ T-cells, memory CD8+ T-cells, and pro-inflammatory cytokines. Vaccine. 2009; 27:6939–6949. [PubMed: 19748578]
23. Bhowmick S, Mazumdar T, Sinha R, Ali N. Comparison of liposome based antigen delivery systems for protection against Leishmania donovani. J. Control. Release. 2010; 141:199–207. [PubMed: 19818373]
24. Reddy R, Zhou F, Nair S, Huang L, Rouse BT. In vivo cytotoxic T lymphocyte induction with soluble proteins administered in liposomes. J. Immunol. 1992; 148:1585–1589. [PubMed: 1538138]
25. Collins DS, Findlay K, Harding CV. Processing of exogenous liposome-encapsulated antigens in vivo generates class I MHC-restricted T cell responses. J. Immunol. 1992; 148:3336–3341. [PubMed: 1588035]
26. Wakita D, et al. An indispensable role of type-1 IFNs for inducing CTL-mediated complete eradication of established tumor tissue by CpG-liposome co-encapsulated with model tumor antigen. Int. Immunol. 2006; 18:425–434. [PubMed: 16415100]
27. Popescu MC, et al. A novel proteoliposomal vaccine elicits potent antitumor immunity in mice. Blood. 2007; 109:5407–5410. [PubMed: 17351111]
28. Allen TM, Mumbengegwi DR, Charrois GJ. Anti-CD19-targeted liposomal doxorubicin improves the therapeutic efficacy in murine B-cell lymphoma and ameliorates the toxicity of liposomes with varying drug release rates. Clin. Cancer. Res. 2005; 11:3567–3573. [PubMed: 15867261]
29. Cashion MP, Long TE. Biomimetic Design and Performance of Polymerizable Lipids. Accounts of Chemical Research. 2009; 42:1016–1025. [PubMed: 19453103]
30. Hotz J, Meier W. Vesicle-templated polymer hollow spheres. Langmuir. 1998; 14:1031–1036.
31. Mahadevan S, Tappel AL. Lysosomal lipases of rat liver and kidney. J. Biol. Chem. 1968; 243:2849–2854. [PubMed: 5653176]
32. Papahadjopoulos D, Nir S, Duzgunes N. Molecular mechanisms of calcium-induced membrane fusion. J. Bioenerg. Biomembr. 1990; 22:157–179. [PubMed: 2139437]
33. Zauner W, Farrow NA, Haines AM. In vitro uptake of polystyrene microspheres: effect of particle size, cell line and cell density. J. Control. Release. 2001; 71:39–51. [PubMed: 11245907]
34. Mohammed AR, Bramwell VW, Coombes AG, Perrie Y. Lyophilisation and sterilisation of liposomal vaccines to produce stable and sterile products. Methods. 2006; 40:30–38. [PubMed: 16997711]
35. Girard P, et al. A new method for the reconstitution of membrane proteins into giant unilamellar vesicles. Biophys. J. 2004; 87:419–429. [PubMed: 15240476]
36. Lutsiak ME, Robinson DR, Coester C, Kwon GS, Samuel J. Analysis of poly(D,L-lactic-co-glycolic acid) nanosphere uptake by human dendritic cells and macrophages in vitro. Pharm. Res. 2002; 19:1480–1487. [PubMed: 12425465]
37. Huisgen R. Cycloadditions - definition classification and characterization. Angewandte Chemie-International Edition. 1968; 7 321-&.
38. Wang Q, et al. Bioconjugation by copper(I)-catalyzed azide-alkyne [3 + 2] cycloaddition. J. Am. Chem. Soc. 2003; 125:3192–3193. [PubMed: 12630856]

39. Allen TM, Cullis PR. Drug delivery systems: entering the mainstream. Science. 2004; 303:1818–1822. [PubMed: 15031496]
40. Mundargi RC, Babu VR, Rangaswamy V, Patel P, Aminabhavi TM. Nano/micro technologies for delivering macromolecular therapeutics using poly(D,L-lactide-co-glycolide) and its derivatives. J. Control. Release. 2008; 125:193–209. [PubMed: 18083265]
41. Vasir JK, Labhasetwar V. Biodegradable nanoparticles for cytosolic delivery of therapeutics. Adv. Drug. Deliv. Rev. 2007; 59:718–728. [PubMed: 17683826]
42. Gabizon A, et al. Prolonged circulation time and enhanced accumulation in malignant exudates of doxorubicin encapsulated in polyethylene-glycol coated liposomes. Cancer Res. 1994; 54:987–992. [PubMed: 8313389]
43. Kirby C, Gregoriadis G. Dehydration-rehydration vesicles - a simple method for high-yield drug entrapment in liposomes. Bio-Technology. 1984; 2:979–984.
44. Bershteyn A, et al. Polymer-supported lipid shells, onions, and flowers. Soft Matter. 2008; 4:1787–1791. [PubMed: 19756178]
45. McKee AS, Munks MW, Marrack P. How do adjuvants work? Important considerations for new generation adjuvants. Immunity. 2007; 27:687–690. [PubMed: 18031690]
46. Mata-Haro V, et al. The vaccine adjuvant monophosphoryl lipid A as a TRIF-biased agonist of TLR4. Science. 2007; 316:1628–1632. [PubMed: 17569868]
47. Porgador A, Yewdell JW, Deng Y, Bennink JR, Germain RN. Localization, quantitation, and in situ detection of specific peptide-MHC class I complexes using a monoclonal antibody. Immunity. 1997; 6:715–726. [PubMed: 9208844]
48. Sallusto F, Geginat J, Lanzavecchia A. Central memory and effector memory T cell subsets: function, generation, and maintenance. Annu. Rev. Immunol. 2004; 22:745–763. [PubMed: 15032595]
49. Yadava A, et al. A novel chimeric Plasmodium vivax circumsporozoite protein induces biologically functional antibodies that recognize both VK210 and VK247 sporozoites. Infect. Immun. 2007; 75:1177–1185. [PubMed: 17158893]
50. Ellman GL. Tissue sulfhydryl groups. Arch. Biochem. Biophys. 1959; 82:70–77. [PubMed: 13650640]

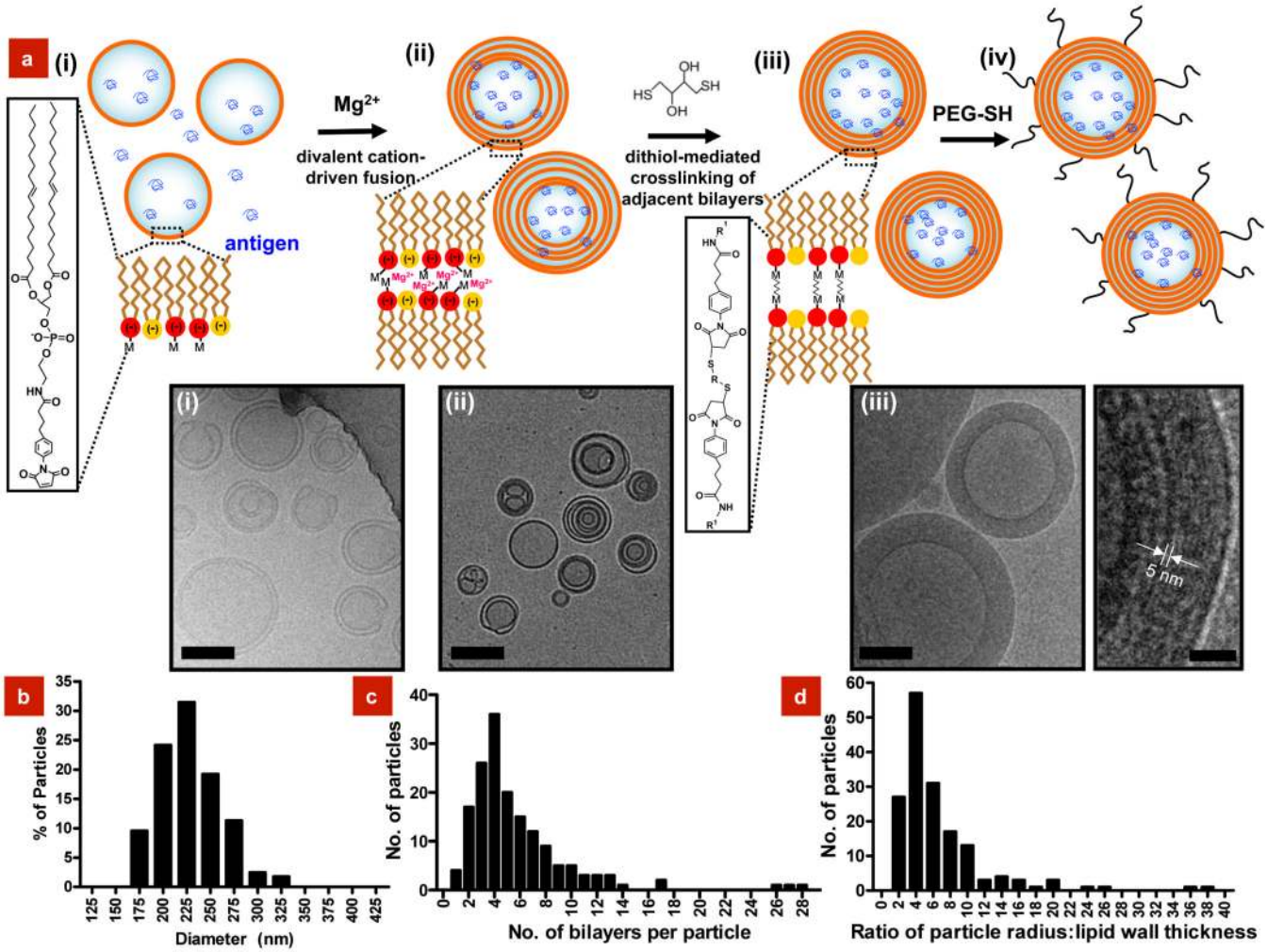

Figure 1. Synthesis of interbilayer-crosslinked multilamellar vesicles (ICMVs)

a, Schematic illustration of ICMV synthesis and cryoelectron microscope images: (i) Anionic, maleimide-functionalized liposomes are prepared from dried lipid films, (ii) divalent cations are added to induce fusion of liposomes and the formation of MLVs, (iii) membrane-permeable dithiols are added, which crosslink maleimide-lipids on apposed lipid bilayers in the vesicle walls, and (iv) the resulting lipid particles are PEGylated with thiol-terminated PEG. Cryo-EM images from each step of the synthesis show (i) initial liposomes, (ii) MLVs, and (iii) ICMVs with thick lipid walls. Scale bars = 100 nm. Right-hand image of (iii) shows a zoomed image of an ICMV wall, where stacked bilayers are resolved as electron-dense striations; scale bar = 20 nm. **b**, ICMV particle size histogram measured by dynamic light scattering. **c, d**, Histograms of ICMV properties from cryo-EM images show **(c)** the number of lipid bilayers per particle, and **(d)** the ratio of particle radius to lipid wall thickness. (n = 165 particles analyzed).

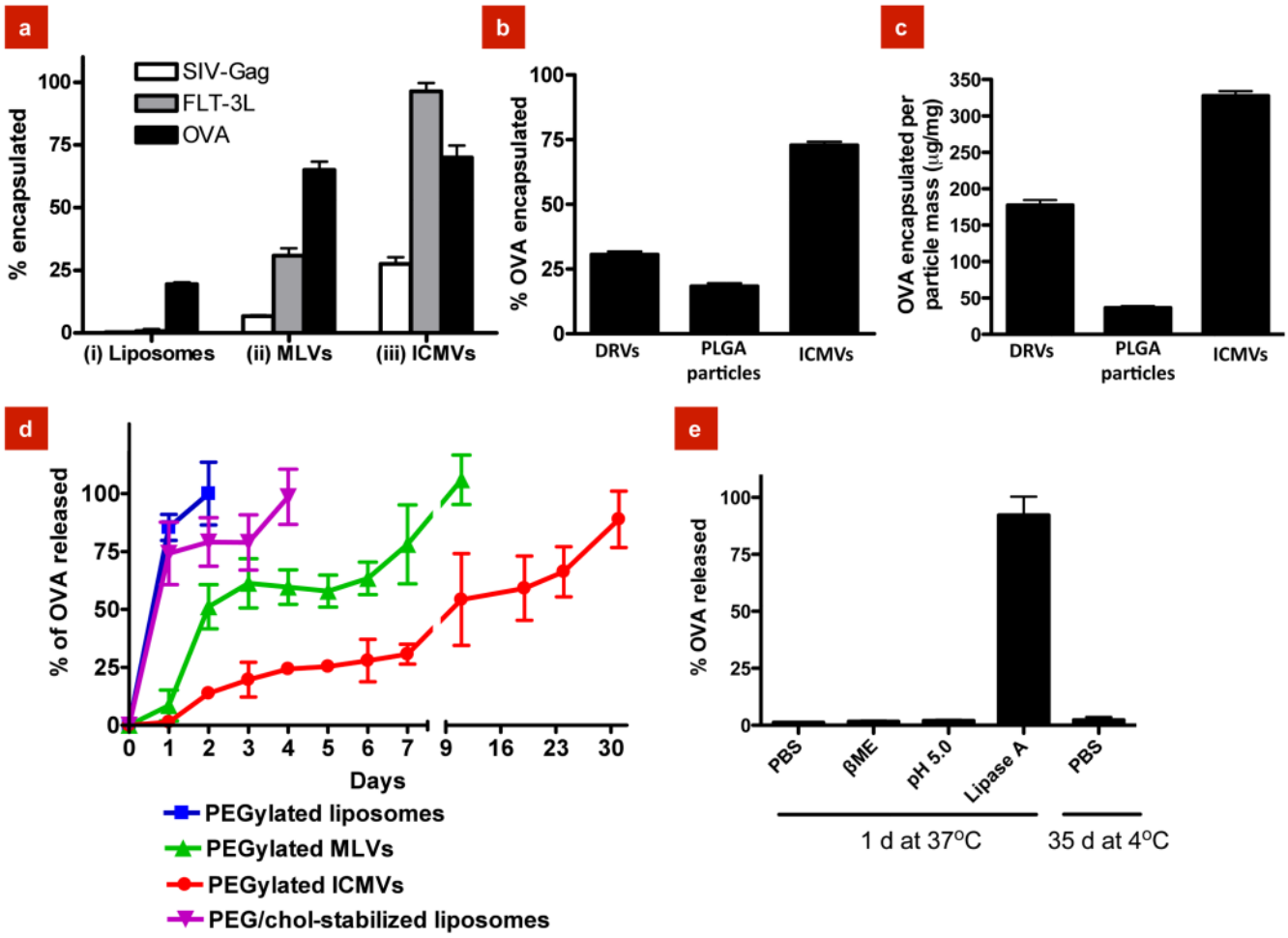

Figure 2. Protein encapsulation and release from ICMVs

a, Encapsulation efficiency of the globular proteins SIV-gag, FLT-3L, or OVA in lipid vesicles collected at each step of ICMV synthesis. **b, c,** Comparison of OVA encapsulation efficiency **(b)**, and total protein loading per particle mass **(c)** in ICMVs vs. dehydration-rehydration vesicles (DRVs) or PLGA nanoparticles. **d,** Kinetics of OVA release from simple liposomes, MLVs, or ICMVs (all with base lipid composition 4:5:1 DOPC:MPB:DOPG) incubated in RPMI medium with 10% serum at 37°C measured over 30 days *in vitro*. Also shown for comparison are release kinetics for liposomes stabilized with cholesterol and PEG-lipid (38:57:5 DOPC:chol:PEG-DOPE). **e,** Release of OVA from ICMVs was measured in buffers simulating different aspects of the endolysomal environment: reducing buffer, 100 mM β-mercaptoethanol (β-ME) in PBS; acidic buffer, 50 mM sodium citrate pH 5.0; lipase-containing buffer, 500 ng/mL lipase A in PBS. Data represent the mean ± s.e.m of at least three experiments with n = 3.

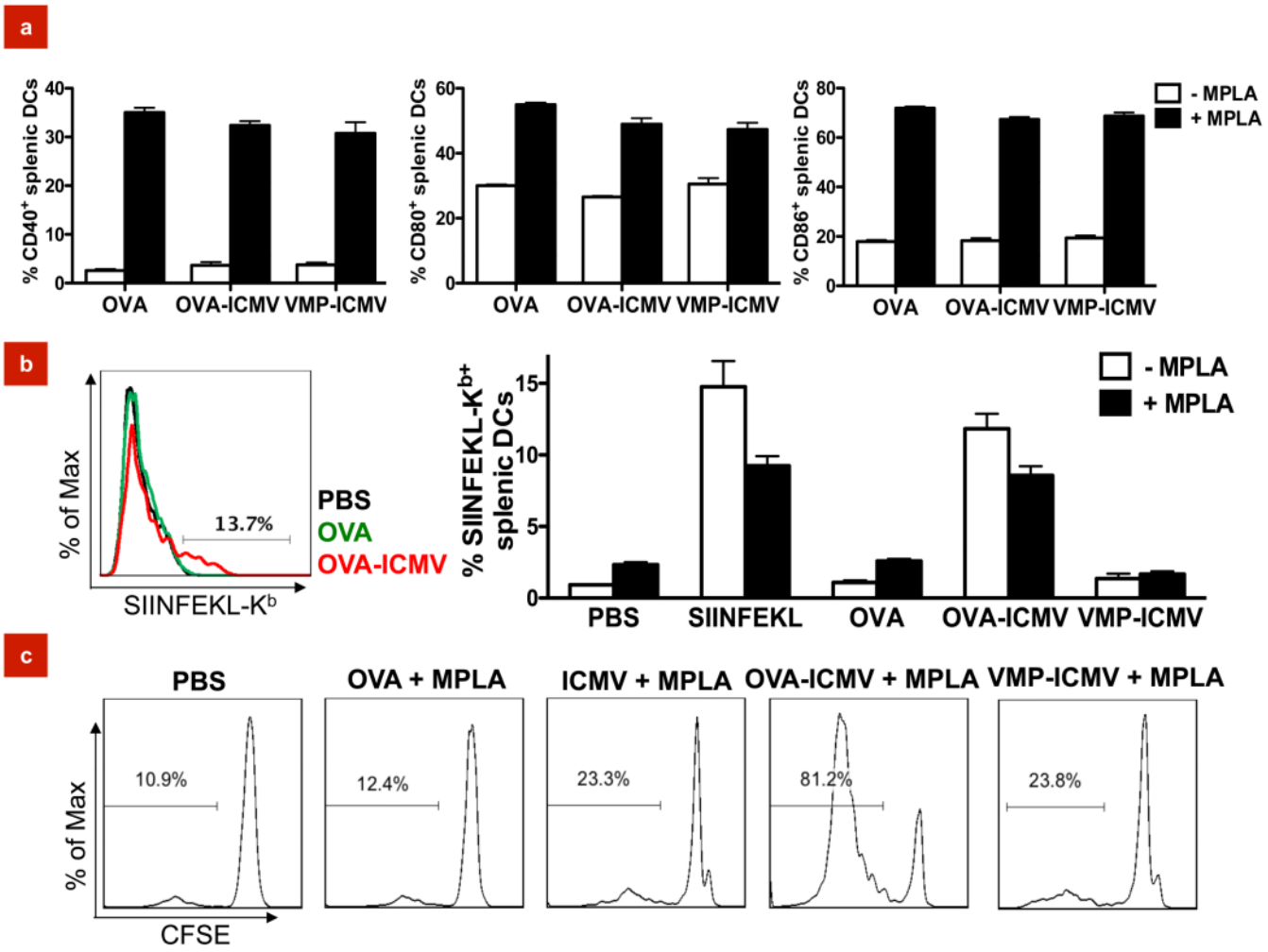

Figure 3. *In vitro* stimulation of immune responses by ICMVs supplemented with the TLR agonist MPLA

a, Flow cytometry analysis of expression of the cell surface costimulatory markers CD40, CD80, and CD86 on splenic dendritic cells (DCs) after 18 hr incubation with 0.7 μg/mL soluble OVA, equivalent doses of OVA loaded in ICMVs, or ICMVs loaded with an irrelevant protein (vivax malaria protein, VMP), in the presence or absence of 0.1 μg/mL MPLA. **b,** Splenic DCs were incubated for 18 hr with 10 μg/mL SIINFEKL peptide ($OVA_{257–264}$), 5.0 μg/mL soluble OVA, equivalent doses of OVA loaded in ICMVs, or VMP-loaded ICMVs in the presence or absence of 0.05 μg/mL MPLA, and the extent of cross-presentation of OVA was assessed by flow cytometry analysis of cells stained with the 25-D1.16 mAb that recognizes SIINFEKL complexed with H-$2K^b$. **c**, 5-(6)-carboxyfluorescein diacetate succinimidyl diester (CFSE)-labeled OVA-specific naïve OT-I $CD8^+$ T-cells were co-cultured with syngeneic splenic DCs pulsed with soluble 0.7 μg/mL OVA mixed with 0.1 μg/mL MPLA, or equivalent doses of OVA-loaded ICMVs mixed with MPLA. Empty ICMVs without antigen or ICMVs loaded with the irrelevant antigen VMP were included as negative controls. Proliferation of $CD8^+$ T-cells was assessed on day 3 by flow cytometry analysis of the dilution of CFSE in the OT-I $CD8^+$ T-cells; shown are histograms of CFSE fluorescence. Gates on each histogram indicate the percentage of divided cells in each sample. Data represent the mean ± s.e.m of at least three experiments with n = 3–4.

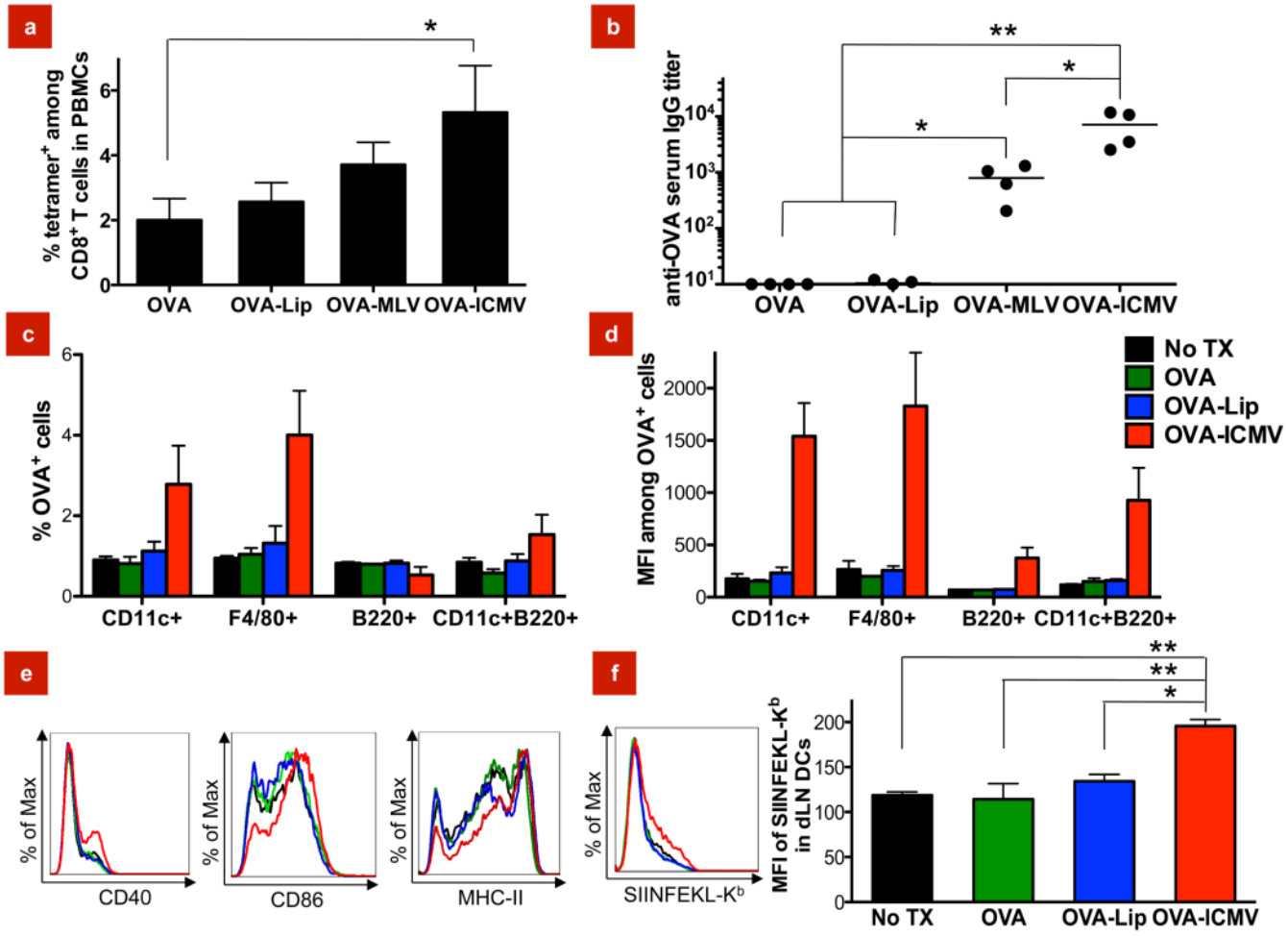

Figure 4. ***In vivo*** **immunization with ICMVs vs. soluble antigen or antigen encapsulated in non-crosslinked vesicles**

a, b, C57Bl/6 mice were immunized s.c. with a single injection of 10 μg OVA delivered in soluble, liposomal, MLV, or ICMV formulations, each mixed with 0.1 μg of MPLA. **a**, The percentage of antigen-specific $CD8^+$ T-cells was determined by flow cytometry analysis of peripheral blood mononuclear cells (PBMCs) 7 days post immunization with fluorescent OVA peptide-MHC tetramers. **b,** Sera from the immunized mice were analyzed by ELISA 21 days post immunization for OVA-specific IgG. **c, d,** C57Bl/6 mice were injected with 10 μg of fluorophore-conjugated OVA mixed with 0.1 μg of MPLA as a soluble, liposomal, or ICMV formulation, and the draining inguinal lymph node (dLN) cells that internalized OVA were assessed on day 2. **c,** Shown are percentages of DCs ($CD11c^+$), macrophages ($F4/80^+$), B cells ($B220^+$), and plasmacytoid DCs ($CD11c^+B220^+$) positive for OVA uptake, and **d,** the mean fluorescence intensity (MFI) of OVA^+ populations. **e, f,** C57Bl/6 mice were injected with 10 μg of OVA mixed with 0.1 μg of MPLA as a soluble, liposomal, or ICMV formulation, and 2 d later, DCs isolated from draining inguinal LNs were analyzed by flow cytometry to assess DC activation and antigen cross-presentation. **e,** Overlaid histograms show costimulatory markers (CD40 and CD86) and MHC-II expression in DCs. **f,** The left panel shows overlaid histograms of inguinal LN DCs stained for SIINFEKL-K^{b+} complexes, and mean MFI levels are shown on the right panel. Data represent mean ± s.e.m of 2–3 independent experiments conducted with n = 3–4. *, $p < 0.05$ and **, $p < 0.01$, analyzed by one-way ANOVA, followed by Tukey's HSD.

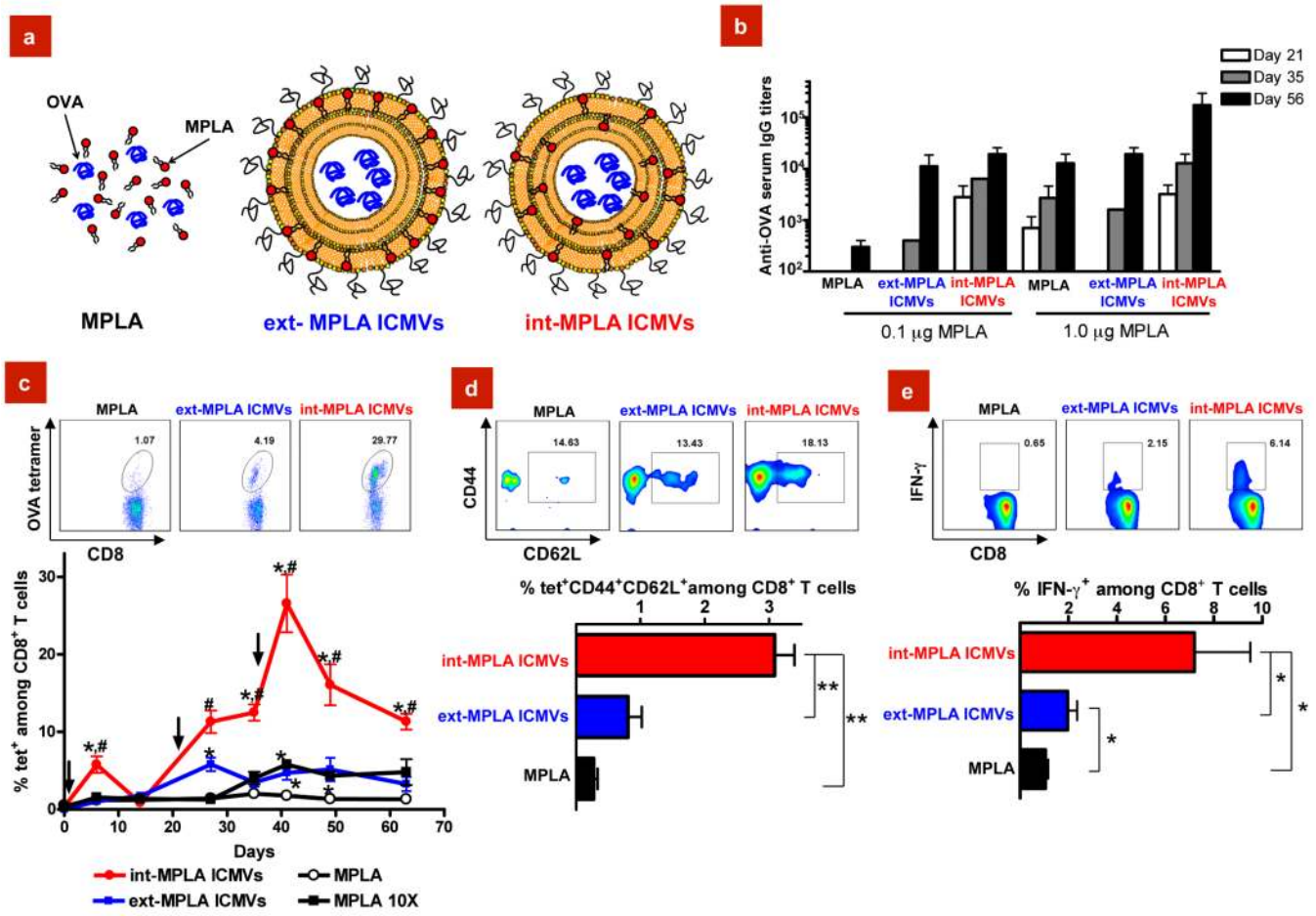

Figure 5. ICMVs carrying antigen in the aqueous core and MPLA embedded in the vesicle walls elicit potent antibody and CD8$^+$ T-cell responses

a, Schematic illustration of the vaccine groups: soluble OVA mixed with MPLA (MPLA), OVA-loaded ICMVs with MPLA only on the external surface (ext-MPLA ICMVs), or OVA-loaded ICMVs with MPLA throughout the lipid multilayers (int-MPLA ICMVs). **b–g,** C57Bl/6 mice were immunized on days 0, 21, and 35 at tail base s.c. with 10 μg OVA and either 0.1 μg or 1.0 μg of MPLA formulated either as MPLA, ext-MPLA ICMVs, or int-MPLA ICMVs. **b,** ELISA analysis of total OVA-specific IgG in sera. **c,** Frequency of OVA-specific T-cells in peripheral blood assessed over time via flow cytometry analysis of tetramer$^+$CD8$^+$ T-cells for vaccinations with 10 μg OVA and 0.1 μg MPLA. Response to vaccinations with soluble OVA + 1 μg MPLA (MPLA 10X) also shown for comparison. Shown are representative flow cytometry scatter plots from individual mice at d41 and mean tetramer$^+$ values from groups of mice vs. time. **d,** Analysis of T-cell effector/effector memory/central memory phenotypes in peripheral blood by CD44/CD62L staining on tetramer$^+$ cells from peripheral blood on d41. Shown are representative cytometry plots from individual mice and mean percentages of tet$^+$CD44$^+$CD62L$^+$ cells among CD8$^+$ T-cells at d41. **e,** Functionality of antigen-specific CD8$^+$ T-cells was assayed on d49 with intracellular IFN-γ staining after *ex vivo* restimulation of PBMCs with OVA peptide *in vitro*. Representative flow cytometry histograms of IFN-γ$^+$CD8$^+$ T-cells from individual mice and mean results from groups are shown. Data represent the mean ± s.e.m of two independent experiments conducted with n = 3. **c,** *, $p < 0.05$ compared to sol OVA + MPLA and #, $p <$

0.05 compared to ext-MPLA ICMVs. **d, e,** *, $p < 0.05$ and **, $p < 0.01$, analyzed by two-way ANOVA, followed by Tukey's HSD.

Table 1

Particle characterization at each step of ICMV synthesis

Synthesis step (Fig. 1a)	Samples	Hydrodynamic diameter[a] (nm)	Polydispersity index	Zeta potential (mV)	Diameter after 7 days in 4°C (nm)	Diameter after lyophilization (nm)	Diameter after lyophilization with 3% sucrose (nm)	Fraction of lipid surface-exposed[b]
(i)	Liposomes	192 ± 39	0.385 ± 0.11	–0.141 ± 0.44	N/A	N/A	N/A	0.37 ± 0.023
(ii)	Mg^{2+}-fused MLVs	220 ± 26	0.217 ± 0.053	–0.151 ± 0.67	N/A	N/A	N/A	0.15 ± 0.025
(iii)	ICMVs	244 ± 17	0.223 ± 0.11	–0.415 ± 0.33	1610 ± 570	N/A	N/A	0.19 ± 0.010
(iv)	PEGylated ICMCs	263 ± 20	0.183 ± 0.025	−2.34 ± 0.44	265 ± 27	2960 ± 1800	269 ± 41	N/A

[a] measured by dynamic light scattering (DLS)

[b] Fraction of lipid exposed on the external surface of vesicles decreased after interbilayer-crosslinked as measured by lamellarity assay36.

[*] all values with mean ± SD

Table 2

ICMV particle yield with varying synthesis conditions

Entry	Lipid composition (molar ratio)[a]	Cation[b]	Crosslinker[c]	Yield %[d]
1	DOPC/DOPG/MPB(40:10:50)	$MgCl_2$	DTT	45
2	DOPC/DOPG/MPB(40:10:50)	$CaCl_2$	DTT	50
3	DOPC/DOPG/MPB(40:10:50)	20 mM NaCl	DTT	0
4	DOPC/DOPG/MPB(40:10:50)	$MgCl_2$	-	0
5	DOPC/DOPG/MPB(40:10:50)	-	DTT	0
6	DOPC/DOPG/MPB(40:10:50)	-	15 mM DTT	4
7	DOPC/DOPG/MPB(60:15:25)	$MgCl_2$	DTT	15
8	DOPC/DOPG/MPB(72:18:10)	$MgCl_2$	DTT	0
9	DOPC/DOPG(80:20)	$MgCl_2$	DTT	0
10	DOPC/DOPG/MPB(40:10:50)	$MgCl_2$	DPDPB[e]	48
11	DOPC/DOPG/MPB(40:10:50)	$MgCl_2$	(PEG)-SH_2[f]	3

[a] hydrated with 10 mM bis-tris propane at pH 7.0;

[b] at 10 mM unless noted otherwise;

[c] at 1.15 mM unless noted otherwise

[d] percentage of lipid mass recovered after synthesis and centrifugation at 14,000 × *g* for 4 min

[e] 1,4-Di-[3´-(2´-pyridyldithio)-propionamido]butane (MW 482);

[f] MW 2000